Does microcalcification increase the risk of rupture?

Myriam Cilla[1,2], David Monterde[1], Estefanía Peña[1,2] and Miguel Á Martínez[1,2]

Abstract

Rupture of atherosclerotic plaque, which is related to maximal stress conditions in the plaque among others, is a major cause of mortality. More careful examination of stress distributions in atherosclerotic plaques reports that it could be due to local stress behaviors at critical sites caused by cap thinning, inflammation, macroscopic heterogeneity, and recently, the presence of microcalcifications. However, the role of microcalcifications is not yet fully understood, and most finite element models of blood vessels with atheroma plaque ignore the heterogeneity of the plaque constituents at the microscale. The goal of this work is to investigate the effect of microcalcifications on the stress field of an atheroma plaque vessel section. This is achieved by performing a parametric finite element study, assuming a plane strain hypothesis, of a coronary artery section with eccentric atheroma plaque and one microcalcification incorporated. The geometrical parameters used to define and design the idealized coronary plaque anatomy and the microcalcification were the fibrous cap thickness and the microcalcification ratio, angle and eccentricity. We could conclude that microcalcifications should be considered in the modeling of this kind of problems since they cause a significant alteration of the vulnerable risk by increasing the maximum maximal principal stress up to 32%, although this increase of stress is not uniform (12% on average). The obtained results show that the fibrous cap thickness, the microcalcification ratio and the microcalcification eccentricity, in combination with the microcalcification angle, appear to be the key morphological parameters that play a determinant role in the maximal principal stress and accordingly in the rupture risk of the plaque.

Keywords

Parametric finite element analysis, vulnerable plaque, coronary disease, microcalcifications, hyperelastic material

Introduction

Atherosclerotic cardiovascular diseases take a huge toll on the society, making them the leading cause of death in developed countries.[1] This vascular disease affects medium- and large-sized arteries, involving the formation of plaques within the artery wall. These plaques result from the accumulation of fat, cholesterol, fibrous, calcific and inflammatory tissue and may cause temporary or definitive lack of blood supply to an organ if the plaque becomes fragile and ruptures.[2]

Although the mechanical factors that promote plaque rupture are not fully understood, plaque stress analysis can provide critical information about the understanding of the plaque rupture mechanism and may eventually provide risk assessment for individual plaque vulnerability. Some authors[3,4] consider peak circumferential stress (PCS) as one of the most important biomechanical factor in the mechanisms leading to rupture of the atherosclerotic plaque, and it has often been used as a predictor of atherosclerotic plaque rupture location. Traditionally, coronary atheroma plaques with a thin fibrous cap thickness and high stenosis ratio have been considered as prone to rupture. However, several pathological and biomechanical studies have provided morphological descriptions of the vulnerable risk, and they conclude that the fibrous cap thickness alone is not a sufficiently accurate predictor for plaque stability. The lipid core length and width are also very important parameters on vulnerability.[5–7]

[1]Applied Mechanics and Bioengineering, Aragón Institute of Engineering Research, University of Zaragoza, Zaragoza, Spain
[2]CIBER-BBN-Centro de Investigación en Red en Bioingeniería, Biomateriales y Nanomedicina, Zaragoza, Spain

Corresponding author:
Miguel Á Martínez, Applied Mechanics and Bioengineering, Aragón Institute of Engineering Research (I3A), University of Zaragoza, María de Luna, s/n. E-50018 Zaragoza, Spain.
Email: miguelam@unizar.es

Nevertheless, apart from plaque morphology, there are other factors that could play a key role in the initiation of failure. For instance, the presence of calcium, which is a common phenomenon, also appears to have an important role in the evolution of atherosclerosis. Initially, the calcium deposits develop in the form of both intracellular and extracellular granules. After that, these granules can either join into large deposits or remain as dispersed collections of microcalcifications that form in the arterial wall.[8] Plaque calcifications both in intravascular ultrasound (IVUS) and in multislice computed tomography (MSCT) are easily recognized. However, small microcalcifications might be missed on MSCT due to its lower resolution.[9] Therefore, there are no reliable means of viewing these microstructures.[10] Only some proposed novel imaging methods could detect the presence of microcalcifications in and around the fibrous cap of plaque lesions.[11–13]

The role of microcalcifications in the mechanics of vulnerable plaque rupture is still debated. Some studies indicate beneficial effects in stabilizing the plaque,[14–16] whereas others suggest that the microcalcifications increase the plaque vulnerability and shift the maximal principal stress (MPS) to the region of the microcalcification.[17–20] Several parametric studies have investigated the effects of varying key parameters that influence stress in diseased arteries.[3,6,7,14,21–24] However, microcalcifications are not usually considered in their studies. Huang et al.[15] tested the hypothesis that calcification impacts biomechanical stresses in human atherosclerotic lesions by fluid–structure interaction (FSI) models. Their conclusion was that calcification does not increase fibrous cap stress in typical ruptured or stable human coronary atherosclerotic lesion. However, their study is related with relatively large calcification areas. Williamson et al.[25] performed a finite element (FE) study to test the sensitivity of predicted levels of stress and strain to the variations of material properties of the atheroma plaque components (normal wall, fibrous plaque, calcified regions and lipid pools). Li et al.[26] implemented a sensitivity study on an idealized two-dimensional (2D) longitudinal cross-section model using FSI simulations. They studied the effect of the fibrous cap thickness and the stenosis degree on the stress in an isolated plaque cap while assuming that the artery walls were rigid. Tang et al.[27] carried out three–dimensional (3D) FSI simulations using modified magnetic resonance imaging data of atherosclerotic plaques with varying lumenal stenosis, cap thickness and material properties. Their sensitivity results indicate that vessel and plaque material properties, plaque structure, component volume and pressure conditions have large impact on stress–strain behaviors. Vengrenyuk et al.[13] performed an FE analysis on a model of patient-specific geometry with three microcalcifications embedded in the cap. The stress around the inclusions was found to increase significantly when the cap thickness was decreased, while the position of the three inclusions was fixed. Similar FSI simulations were performed by Bluestein et al.[17] Wenk[19] investigated the effects of localized regions of microcalcifications on the stress field of atherosclerotic plaque caps in a section of carotid artery using a global sensitivity analysis method known as Sobol indices.[28] They conclude that the maximum MPS always shifted to the region of microcalcification and the amplification of the stress depends on the zone where the microcalcification appears. Maldonado et al.[20] found a great microcalcification influence on the atheroma plaque vulnerability; however, their results could be related to the hard material properties used for the microcalcification tissue.

The main goal of this study is to assess the influence of microcalcifications on the stresses in the fibrous cap using an idealized coronary vessel with one microcalcification included. In addition, we investigate the biomechanical interaction between the most influential parameter of the vessel geometry, the fibrous cap thickness and the size and the position of the microcalcification in the mechanical risk factor of vulnerable plaque. This is accomplished by 108 FE analyses in an idealized parametric coronary vessel model with one microcalcification. The geometrical parameters used to define and design the idealized cross-sectional coronary plaque anatomy and the microcalcification were as follows: (1) the fibrous cap thickness; (2) the microcalcification ratio; (3) the microcalcification angle and (4) the microcalcification eccentricity. Furthermore, a sensitive analysis on MPS to the microcalcification material properties has been performed in order to evaluate the material properties' influence on the results.

Materials and methods

Idealized geometry

An idealized cross-sectional coronary vessel with atheroma plaque was modeled. The model was extruded at a small length in order to introduce some purely 3D parameters such as the fiber orientation due to the anisotropy of the tissue, and plane strain boundary conditions were applied. The basic geometry was built considering a coronary vessel with an external radius of 2 mm and a vessel wall thickness of 0.5 mm. These dimensions as well as the atherosclerotic vessel morphology were obtained from studies by Versluis et al.[4] and Bluestein et al.[17] A circular-shaped lumen was considered, and the atheroma plaques were modeled by a blunt crescent-shaped lipid pool located inside the vessel, which is symmetric with respect to the central cross section.[7,21,29,30] A microcalcification, which was considered as spherical and located in the fibrous cap, was also introduced in the model. The basic geometry was created taking into account both the composition and the dimensions of the tissue (adventitia), the fibrous plaque, the lipid core and the microcalcification. The whole media layer has been considered as fibrotic nonhealthy tissue, whereas the adventitia has been

considered as the only healthy layer of the vessel (see Figure 1).

The microcalcification influence was evaluated by carrying out a parametric study of the geometric factors. ABAQUS 6.10 software was used to perform static FE analyses on 108 idealized plaque morphologies. The geometric parameters analyzed were the following: the fibrous cap thickness (fc); the microcalcification ratio (r), which is obtained by dividing the microcalcification diameter by the fibrous cap thickness, $r(\%) = D(\text{mm})/fc(\text{mm}) \times 100$; the microcalcification position angle (α) and the microcalcification eccentricity (x), which was defined as the ratio between d, being d the distance from the lumen wall to the microcalcification center point, and the fibrous cap thickness (fc), $x(\%) = d(\text{mm})/fc(\text{mm})100$. These parameters were selected for the analysis because of their great influence on the atheroma vulnerability and the microcalcification position and dimensions.[7,18,21,23]

A fine adaptive mesh was created in some regions of the model such as the fibrous cap area and the microcalcification. This mesh was chosen after previous sensitivity analysis, and it consisted of 40,000 linear hybrid tetrahedral elements and 10,000 nodes. The geometrical model, the parameters studied and the mesh used are shown in Figure 1.

The values considered for each parameter are shown in Figure 2. Realistic morphological data were investigated by varying the microcalcification angle ($0° \leqslant \alpha \leqslant 32.5°$), the fibrous cap thickness ($0.05\text{mm} \leqslant fc \leqslant 0.1\text{mm}$), the microcalcification eccentricity ($25\% \leqslant x \leqslant 75\%$) and the microcalcification ratio ($10\% \leqslant r \leqslant 20\%$). The minimum and maximum values of α correspond to the central point of the fibrous cap and the shoulders, respectively.[31,17]

Material model and boundary conditions

All tissues were modeled as nonlinear,[32–34] hyperelastic[35] and incompressible materials.[36,37] The behavior of the lipid core, the atheroma plaque and the vessel wall were modeled by using the strain energy function (SEF) proposed by Gasser et al.[38]

$$\Psi = C_1[I_1 - 3] + \frac{k_1}{2k_2} \sum_{i=4,6} \exp\left(k_2[\kappa[I_1 - 3] + [1 - 3\kappa][I_i - 1]]^2\right) - 1 \quad (1)$$

where $C_1 > 0$ and $k_1 > 0$ are stress-like parameters and $k_2 > 0$ and $0 \leqslant \kappa \leqslant 1/3$ are dimensionless parameters (when $\kappa = 0$, the fibers are perfectly aligned (no dispersion), and when $\kappa = 1/3$, the fibers are randomly distributed and the material becomes isotropic), I_1 is the first invariant of $\mathbf{C} = \mathbf{F}^T\mathbf{F}$ with $\mathbf{F}$ the deformation gradient tensor and $I_4 = \mathbf{m}_0 \cdot \mathbf{C}\mathbf{m}_0$ and $I_6 = \mathbf{n}_0 \cdot \mathbf{C}\mathbf{n}_0$ are invariants that depend on the direction of the family of fibers at a material point $\mathbf{X}$ that is defined by the unit vectors field $\mathbf{m}_0$ and $\mathbf{n}_0$.[39]

The lipid core and the atherosclerotic plaque were modeled as exponential isotropic materials, while healthy wall was considered as an anisotropic material with two families of fibers, oriented at $\pm 61.8°$ with respect to the circumferential direction. Both families of fibers were assumed to have the same mechanical properties.[35] Nevertheless, the behavior of the microcalcification was modeled by using the isotropic Neo-Hookean SEF, $\Psi = C_1[I_1 - 3]$.

The material parameters for the constitutive law of the tissue were obtained using the Levenberg–Marquardt minimization algorithm.[40] The

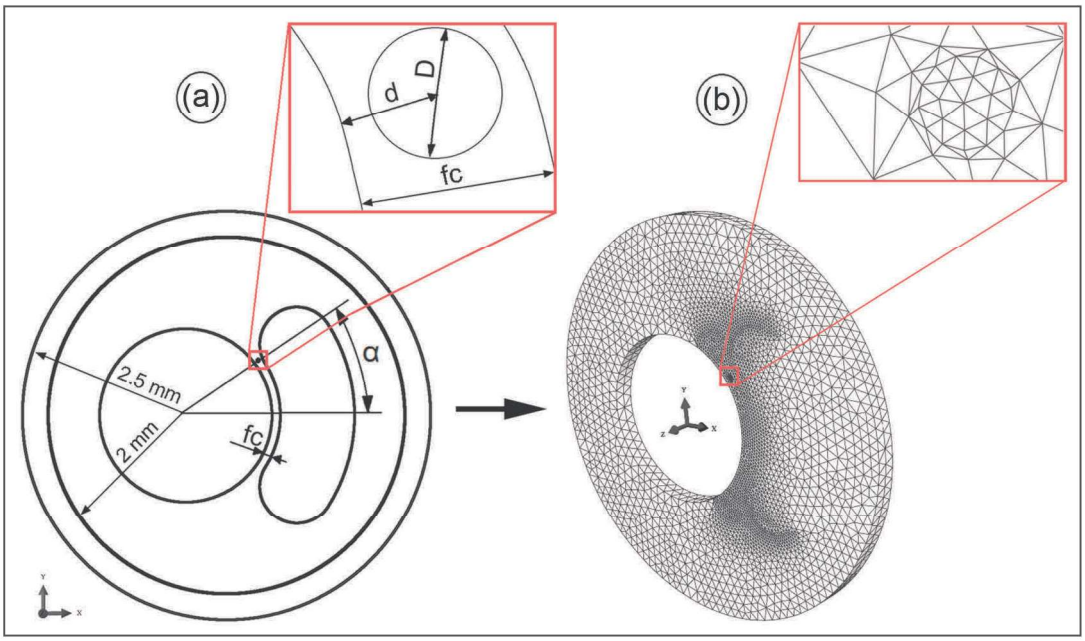

Figure 1. (a) Geometrical parameters shown on the cross-sectional coronary model. (b) Finite element mesh used.

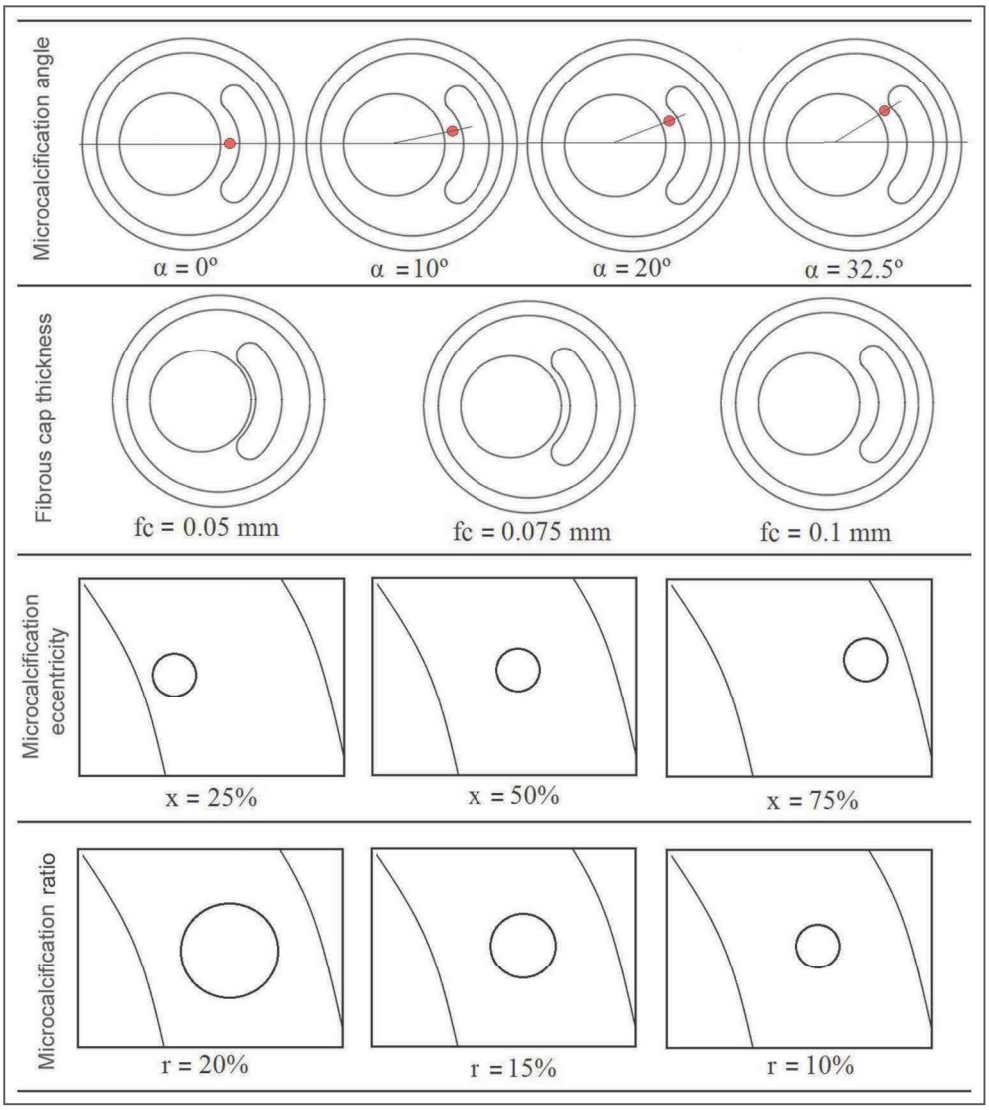

Figure 2. Variations of the geometrical parameters in the parametric models.

Table 1. Material parameters used in the finite element analysis for the adventitia, the atheroma plaque, the lipid core and the microcalcification.

	C_1 (kPa)	k_1 (kPa)	k_2 (-)	κ (-)	ε (-)
Adventitia	8.44	547.67	568.01	0.26	0.041
Atheroma plaque	9.58	17,654.91	0.51	0.33	0.056
Lipid core	0.052	965.76	70	0.33	0.03
Microcalcification	977.3	—	—	—	0.024

experimental data used for the simulations, which were obtained from the previous works, were the following: the adventitia properties from Holzapfel et al.,[35] the plaque and the lipid core properties from Versluis et al.,[4] and finally, the microcalcification properties from Loree et al.[41] Table 1 shows the results of the material parameter identification for each tissue considered.

The goodness of the fit was checked by the normalized mean square root error (ε), which is defined as $\varepsilon = \sqrt{(\chi^2/n-q)}/\mu$, where q is the number of parameters of the SEF, n is the number of data points, $n-q$ is the number of degrees of freedom and μ is the mean stress.

Regarding the boundary conditions, symmetry conditions were imposed in the corresponding symmetry planes. Therefore, only the half of the microcalcification (half of a small sphere) was considered due to the symmetry conditions. The models were solved imposing conditions to reproduce the assumption of plane strains. A constant internal pressure of 140 mmHg

(18.7 kPa) was imposed in the inner surface of the lumen, simulating the blood flow pressure.[23]

MPS was considered as the mechanical factor for the purpose of comparison in this study. Regarding vulnerability of the plaque, different threshold stress values have been proposed by different authors.[3,7,14,41,42] In this study, a threshold value of 247 kPa has been used according to the set of experimental data obtained by Loree et al.[41] supposing a normal distribution of the data.[7] This threshold value indicates that the probability of having plaque rupture is 0.05 for the cases whose combination of parameters has a maximum MPS equal or higher than 247 kPa according to the Loree et al.'s[41] data.

Results

Parametric study

The obtained contour maps can be classified into two main groups according to the influence of including the microcalcification on the results. The first group includes the models in which the geometry without microcalcification has already maximum MPS in the zone where the microcalcification is located. Generally, geometries with small microcalcification angles ($\alpha \leqslant 10°$), the smallest fibrous cap thickness ($fc \leqslant 0.05$ mm) and the small microcalcification eccentricity ($x = 25\%$) belong to this group. In that case, the microcalcification hardly increases the MPS. The second group includes the rest of the models in which microcalcifications are located far away from the maximum MPS. In that case, the microcalcification considerably increases the MPS. Figure 3 illustrates the difference between both the groups. Figure 3(a) shows a case that belongs to the first group where the dimensions are 0.05 mm thickness of fibrous cap, 32.5° of microcalcification angle, 25% of microcalcification eccentricity and 20% of microcalcification ratio. The maximum MPS, which is located at the fibrous cap thickness, does not increase when the microcalcification is considered. Figure 3(b) shows a case belonging to the second group whose dimensions are 0.1 mm thick fibrous cap, 32.5° of microcalcification angle, 75% of microcalcification eccentricity and 20% of microcalcification ratio. The maximum MPS is located in the central part of the fibrous cap in the noncalcified model, but the MPS shifts to the region around the microcalcification in the calcified one. The MPS increases around 40% from the case with microcalcification to the case without.

Maximum MPS for each combination of parameters is shown in Figure 4. For each subfigure that corresponds to each microcalcification angle, there are four surfaces, one for each microcalcification ratio and one for the case without microcalcification. The fibrous cap thickness fc and microcalcification eccentricity x were the variables represented in each surface. All subfigures include the safety threshold plane at a maximum MPS of 247 kPa.

In all cases, the MPS increases slightly as the microcalcification ratio increases, showing a dependency of this parameter on the MPS. As expected, the reduction of the fibrous cap thickness dramatically increases the MPS, showing the relevance of the fibrous cap thickness on MPS.[7] The influence of the microcalcification eccentricity depends on the microcalcification angle; for the small microcalcification angles ($\alpha \leqslant 20°$), the microcalcification eccentricity has no influence on the MPS; however, for long ones ($\alpha > 20°$), the microcalcification located at $x = 75\%$ increases the MPS, while for $x = 25\%$, the microcalcification has a protective effect.

The majority of parameter combinations are above the threshold plane of 247 kPa because the values of the fibrous cap thickness chosen are the most critical and thus vulnerable even without microcalcification included.[7]

Statistical analysis

To assess the influence of the geometrical parameters on the MPS, a statistical analysis was performed. The Lilliefors test (checking the normality of the distribution), the Student's t-tests and the analysis of variance (ANOVA) were used. The Student's t-test was performed at 5% of significance level.

Figure 5 shows the statistical analysis performed on the relative increment of the maximum MPS ratio (ΔMPS) between the model with and without microcalcification, in the critical region (fibrous cap and plaque shoulders)

$$\Delta\text{MPS}(\%) = \frac{\text{MPS with (kPa)} - \text{MPS without (kPa)}}{\text{MPS without (kPa)}} 100 \quad (2)$$

The results of the ANOVA grouped for the different levels of each geometrical parameter studied are presented in Figure 5. The studied parameter becomes influential on the results if the relative increment of MPS is modified significantly when this parameter varies. The ANOVA statistics related to the fibrous cap thickness is shown in Figure 5(a) and proves the influence of this parameter on MPS. The median of each variation of fibrous cap thickness decreases from 19.8% to 8.3% for $fc = 0.05$ and 0.075 mm, respectively, and slightly increases again for $fc = 0.1$ mm. A noteworthy remark is that the presence of microcalcification is more influential for low values of fibrous cap. With regard to microcalcification ratio, the median and dispersion for each variation of the parameter increase slightly as the microcalcification ratio increases (Figure 5(b)). The median of the relative variation of MPS is between 8.8% and 12.3% when the microcalcification ratio varies between 10% and 20%. Microcalcification angle statistical analysis is presented in Figure 5(c), showing that the medians are very similar, taking a value around 10% for all angle values. Finally, for the microcalcification eccentricity, the results show that the

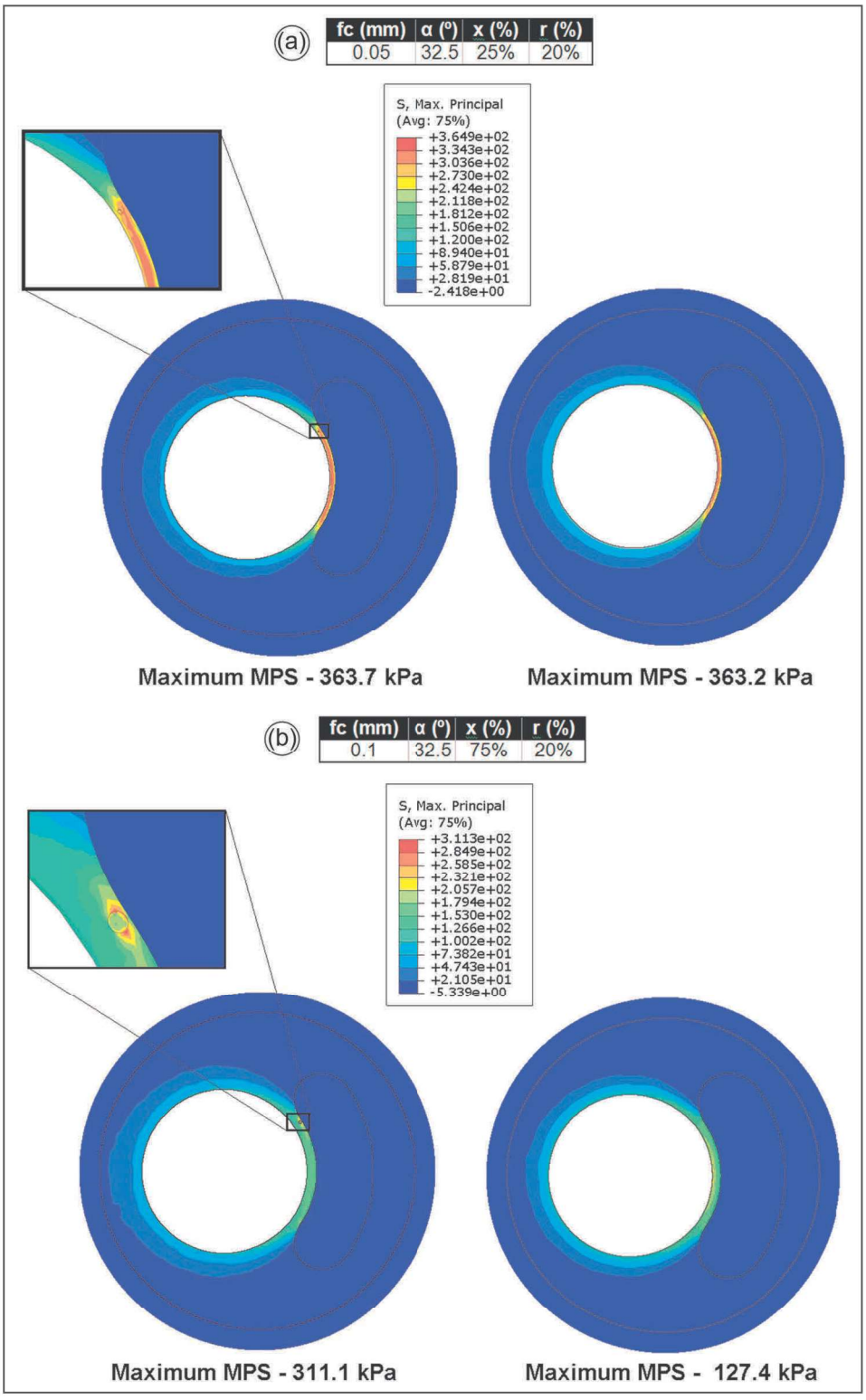

Figure 3. Contour maps of MPS. Comparison between models with and without microcalcification: (a) belongs to the first group where the maximum MPS is located at the fibrous cap thickness in both models and (b) belongs to the second group where the maximum MPS is located in the central part of the fibrous cap in the noncalcified model, but the MPS shifts to the region around the microcalcification in the calcified one.

MPS: maximal principal stress.

medians and dispersion increase as this parameter increases from 9.9% to 16.3% for $x = 25\%$ and 75%, respectively (Figure 5(d)).

The results of the paired Student's t-test performed on the maximum MPS value from the cases with and without microcalcification grouped as exposed in

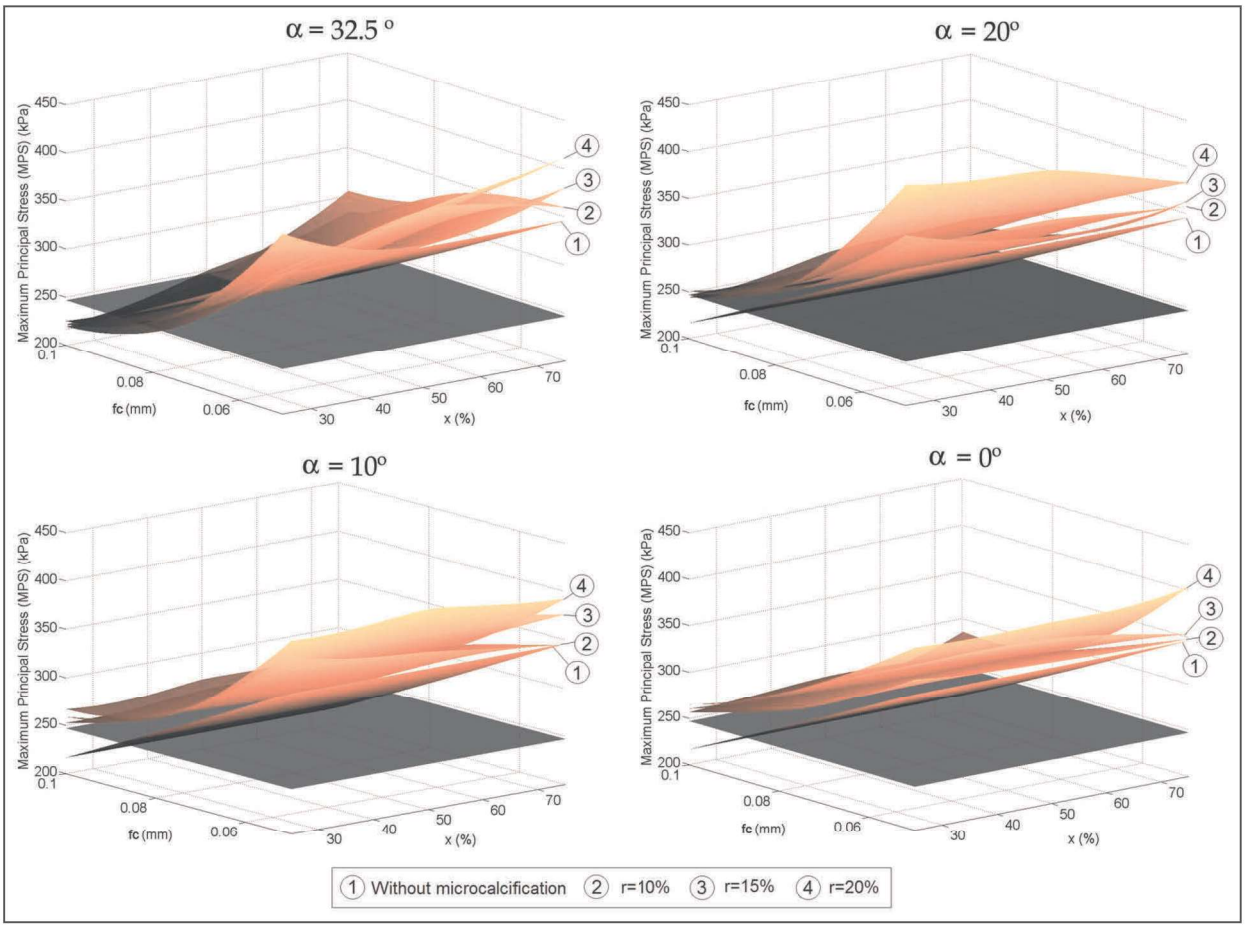

Figure 4. Maximum MPS surfaces for a given microcalcification angle.

Figure 5 are promising. The results of this test are returned in h and p value. $h = 1$ indicates that there are significant differences between both groups at the 5% significance level, and $h = 0$ indicates the rejection of the hypothesis. The p value is the probability of not observing the fact reflected in h (there are no differences between the results with and without microcalcification). All paired Student's t-test performed presents $h = 1$ and $p < 10^{-5}$; thus, there are always significant differences between the cases with and without microcalcification, which indicates the impact of microcalcifications.

Sensitivity of MPS to the microcalcification material properties

A sensitivity analysis of MPS to small changes of microcalcification mechanical properties has been carried out in order to investigate the influence of microcalcification stiffness on the MPS. In the literature, there are a wide range of calcified material properties, and some conclusions presented by other authors could be related to material property values. Note that for the case of a Neo-Hookean material, a relation can be established between C_1 and E, $C_1/2 = E/2(1 + \nu)$, where E is the Young's modulus valid for linear elastic materials and ν the Poisson's ratio, whose value has been considered 0.5 (incompressible material).

In the studies performed by Vengrenyuk et al.,[13] Cheng et al.[14] and Lee et al.,[43] the Young's modulus of calcified was estimated as 10-fold that of plaque E_θ, that is, approximately $C_1 = 6666.6$ kPa (E = 10,000 kPa) for the calcified areas. The experimental analysis performed by Loree et al.,[41] on which our study and many others works in the literature are based,[15,17,25,27] reported $C_1 = 977.3 \pm 856$ kPa (E = 1466 ± 1284 kPa) for the calcified tissue. Similar results were found by Beattie et al.[44] ($C_1 = 2660$ kPa or E = 3990 kPa) for the calcification tissue. Holzapfel et al.[45] modeled in their study the calcification as a rigid body; however, in a later article of the same authors,[46] they performed their own experiments, and the microcalcification properties obtained were $C_1 = 8400 \pm 3133.3$ kPa (E = 12,600 ± 4700 kPa), after that Wong et al.[16] among other authors used these results to carry out their studies. Kiousis et al.[47] used to characterize the calcified mechanical behavior $C_1 = 90,000$ kPa (E = 135,000 kPa). Finally, Maldonado et al.[20] accomplished their study with stiff calcified material properties ($C_1 = 6.6$ GPa or E = 10 GPa).

Viewing this wide range of calcified material parameters, the sensitive analysis has been performed by

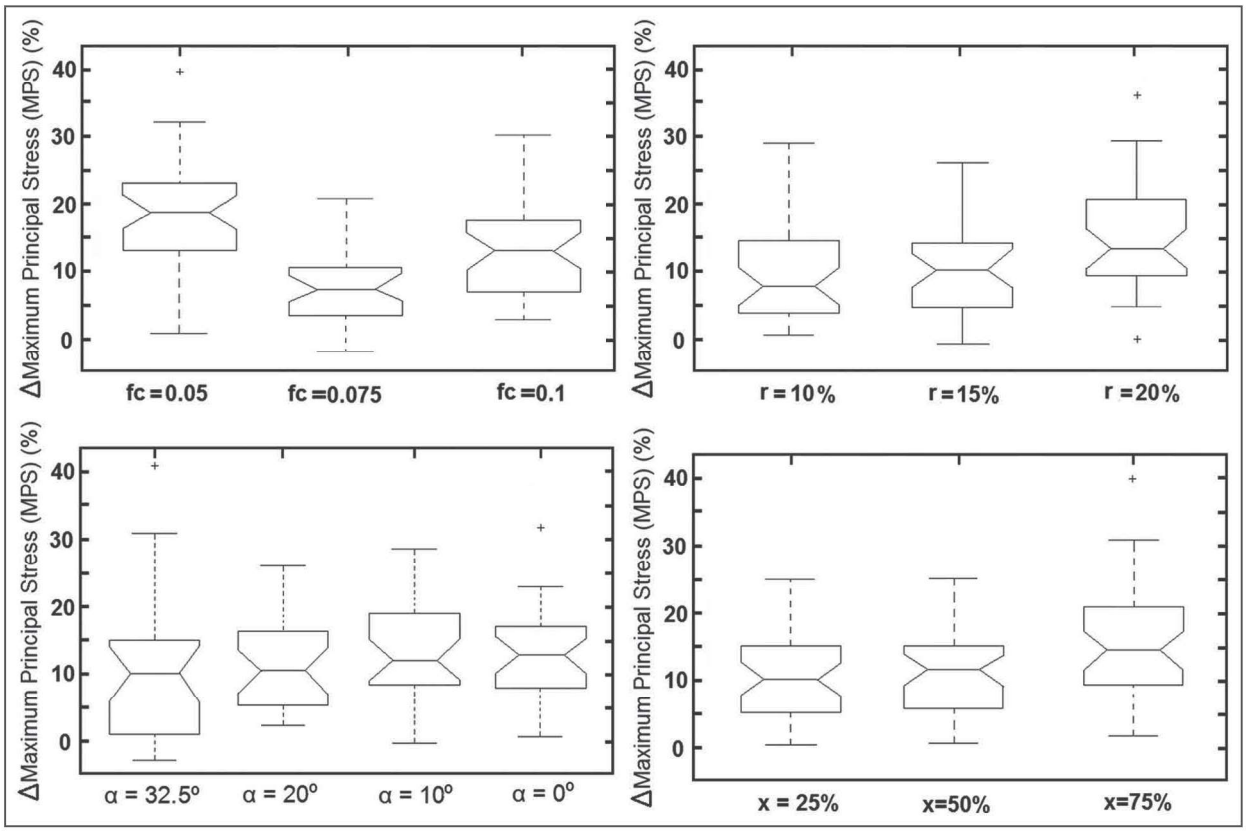

Figure 5. ANOVA statistics: relative increment of maximum MPS (ΔMPS) versus the variation of each parameter. On each box, the central mark is the median, the edges of the box are the 25th and 75th percentiles, the whiskers extend to the most extreme data points not considered outliers and outliers are plotted individually. It should be noted that statistically differences were found between all the considered groups.

varying the initial values of C_1. The constant C_1 has been varied 100 and 10,000 times higher than that proposed by Loree et al.[41] and used in our study ($C_1 = 977.3$ kPa, which corresponds to E = 1465.95 kPa). Thus, the values of C_1 used to perform the sensitivity analysis are 977.3, 9.773×10^4 and 9.773×10^6 kPa. These analysis have been performed on a representative geometry with the following dimensions: 0.05 mm of fibrous cap thickness, 20% of microcalcification ratio, 0° of microcalcification angle and 50% of microcalcification eccentricity. Figure 6 shows the results obtained for the sensitive analyses to the microcalcification material properties. The MPS field for the different microcalcification material properties considered is shown on a zoom detail of the microcalcification area around. The results show that MPS amplitude increases dramatically as the stiffness increases, and the way in which the soft tissue works also changes. For $C_1 = 977.3$, the microcalcification is mainly under tensile stresses (344.1 kPa) and the compressive stresses are neglected (4.87 kPa); this fact allows the deformation of the microcalcification. However, for C_1 values of 9.773×10^4 and 9.773×10^6 kPa, the microcalcification is under compressive and tensile stresses, which restricts the microcalcification deformation. The tensile stress increases until 1256 and 1300 kPa for C_1 values of 9.773×10^4 and 9.773×10^6 kPa, respectively, and the compressive stress reaches 676.4 and 725.4 kPa, respectively. Such results indicate that deviation in the microcalcification material constant value would modify the conclusions regarding the influence of the microcalcifications on plaque vulnerability.

Discussion

In this study, the presence of microcalcifications in the fibrous cap of an atheroma plaque vessel was investigated using a plane strain FE model. We can conclude from the obtained results that the dimensions and location of the microcalcification had a significant influence on the magnitude of stress in the fibrous cap. In some cases, the presence of microcalcification increases the MPS by up to 40% when compared with the case without it. However, this increase of MPS is not uniform for all cases (12% on average). The influence of the microcalcification on the magnitude of MPS depends on the location of MPS in the noncalcified case. It was found that when the microcalcification is located in a region where the MPS of the model without microcalcification appears, the influence of the microcalcification is not as much important. Nevertheless, if the microcalcification is located in a region far from the maximum

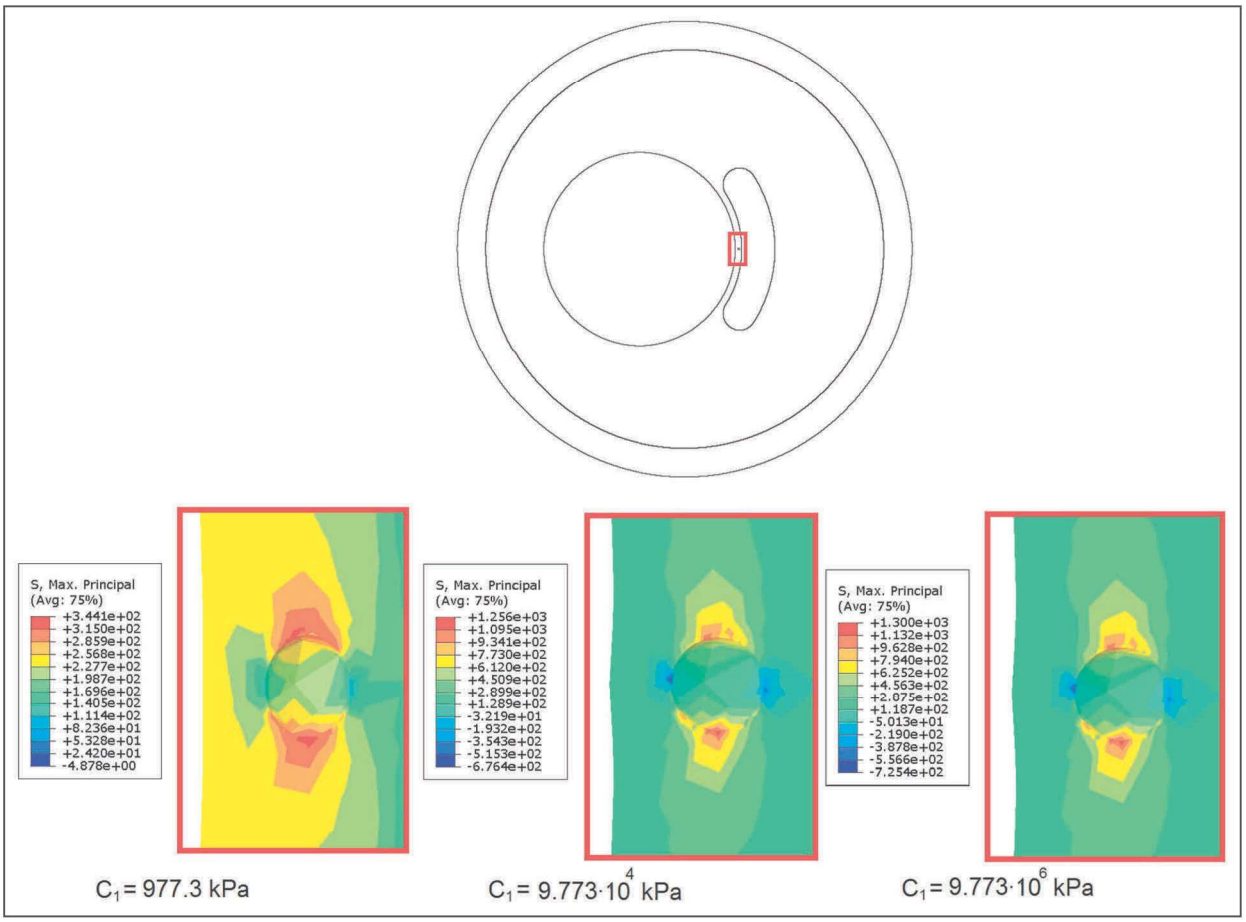

Figure 6. Sensitive analyses of MPS to the microcalcification material properties. The constant C_1 has been varied 100 and 10,000 times higher than that used in our study ($C_1 = 977.3$), that is, 977.3, 9.773×10^4 and 9.773×10^6 kPa for the microcalcification tissue.

MPS in the equivalent noncalcified plaque, the MPS shifts around to the microcalcification and the global value of MPS increases considerably (see Figure 3).

Historically, fibrous cap thickness has been considered the most important and almost the exclusive factor determining plaque vulnerability.[48,49] To date, very few computational studies have been performed specifically to investigate the effect of other parameters of the geometry in a model with microcalcifications included. It has been shown in the literature that microcalcifications can have a significant effect on the stress in fibrous caps.[13,17,18,20,26] However, the main difference between this study and previous works in the literature is an additional focus on the effects of both the dimensions and the location of a microcalcification by using a parametric model. The results of this work predict a significant increase in MPS due to variations of the fibrous cap thickness. However, the influence of other parameters such as the microcalcification ratio, angle and eccentricity has also been found significant. As shown in Figure 4 and its statistical analysis (Figure 5), the fibrous cap thickness is the most influential parameter on MPS, and the MPS increases as this parameter decreases reaching $\Delta MPS = 19.8\%$ for $fc = 0.05$ mm. The MPS increases slightly as the microcalcification ratio, angle and eccentricity increase. The influence of the microcalcification eccentricity is different according to the microcalcification angle; for the small microcalcification angles ($\alpha \leqslant 20°$), the microcalcification eccentricity has no influence on the MPS; however, for the long ones ($\alpha > 20°$), the microcalcification located at $x = 75\%$ increases the MPS.

However, the influence of microcalcification on the MPS of this study and others of the literature[13–15,17,20,25,27,43,45,47] could be affected by the calcified material properties defined, as shown in the results of the sensitivity analysis performed on the microcalcification material properties. According to our results, the stress state around the microcalcification highly depends on the relative stiffness of both materials. While for a low C_1 microcalcification parameter, only tensile stresses appear in circumferential direction, when C_1 increases, a high compression occurs in radial direction, and an abrupt increment is produced in the tensile circumferential stress.

Some limitations of this study are as follows. First, the use of an idealized plane strain geometry does not fully capture the complexity of the plaque lesion. Several studies have demonstrated the performance and importance of 3D models to identify vulnerable plaques

accurately.[3,7,16] Cilla et al.[7] analyzed the performance of 2D plane strain plaque models versus 3D models, concluding that plane strain plaque models are not accurate enough to calculate MPS distribution since these models overestimate the maximum MPS. However, although their study proved that the maximum MPS varies from 3D to 2D plane strain geometries, similar trends of the relative influence of each geometrical parameter on the MPS were found. Furthermore, the authors performed previous tests in an idealized 3D model with a microcalcification, and very similar results were found about the influence of the microcalcifications. The fact of considering 3D or 2D plane strain models should affect the obtained absolute maximum MPS; however, this study is based on the relative values of the MPS, that is, ratio between the maximum MPS with or without microcalcification. And these relative measures of the MPS do not vary from 3D to 2D plane strain analysis. Moreover, an idealized straight geometry with just one spherical microcalcification has been used to perform the parametric analysis in order to simplify the study and to clearly detect the isolated influence of each parameter. Probably, there will be more than one of such spot in a real case. However, the inclusion of more microcalcifications would involve the addition of more parameters to define the localization of each new microcalcification. As the number of parameters increases, the clarity of the study could decrease. An excessive number of parameters could obstruct the assessing of each individual parameter appearing complex cross correlations amongst them and conducting to confused final conclusions. It has been observed that the increase of MPS due to the microcalcification presence is very local, that is, the stress increases only very close to the microcalcifications. Therefore, we estimate that the presence of several microcalcifications would not affect the obtained conclusions for one isolated microcalcification. Second, viscoelastic effects were not considered.[50,51] It is well known that blood vessels exhibit viscoelastic properties, and some authors such as Saito et al.[52] have demonstrated the importance of including these effects, especially for FSI analysis; however, the assumption of negligible viscoelastic response in arterial walls has been routinely made in the analysis of blood vessel dynamics.[3,4,23] Moreover, the influence of residual stress has been ignored in this study[53] due to the difficulty of estimation in real geometries.[54] Cilla et al.[7] demonstrated the importance of considering residual stresses in arterial models to get an accurate calculation of the stress distribution through the arterial wall, obtaining that the maximum MPS varies when the residual stress are considered but following the same general trend of the results. Furthermore, to the best of the authors' knowledge, there are no available data in the literature of the local stresses occurring by the microcalcification presence. Third, since microcalcifications are small defects, homogenization methods could be used to perform the analysis; however, the most important microscopic components should also be included, as well as its spatial distribution and interactions, which is out of the scope of this work. Moreover, the dimensions of the microcalcification are some orders of magnitude over the microscale of the main load-bearing microstructural components. Finally, the analysis does not reproduce the pulsatile nature of physiological blood pressure. Also, the FSI effects resulting from such cyclic loading were not considered.[55] Nevertheless, it has been documented that the effect of fluid shear stress is insignificant when compared to the effect of tensile wall stresses as a direct component in plaque fracture dynamics,[15,56] although it is considered essential in plaque formation and growth. The estimation of stresses induced by the static pressure load has been proved to be valid to identify stress concentrations in atherosclerotic lesions[14] since the location of stress concentration does not significantly differ between models including static pressure and models with complex dynamic pressure profiles. Additionally, all these limitations could probably contribute to modify the local wall stress amplitudes. However, the purpose of this study is to compare the maximum MPS occurring in models with and without microcalcifications in order to assess the influence of it on the obtained stress. The inclusion of the features named above should not influence on the final conclusion since models with and without microcalcifications have been computed under the same conditions and relative measures of the MPS have been compared. Moreover, the calculation of a highly accurate MPS distribution, including all the advanced features, in order to detect the vulnerable areas and limits in an atherosclerosis model with a microcalcification included is out of the scope of this work.

Calcification is commonly found in atherosclerosis, and the presence and extent of calcification are usually associated with worse prognosis.[57] However, the impact of calcification within a specific atherosclerotic lesion is still unclear. Despite these limitations, this study shows that microcalcifications could cause an important increase in peak stress, but it might depend on other geometrical factors that also affect the location of points of maximum stress. These results have potential implications for the estimation of interventions for coronary artery disease, and they can be considered as an additional step toward the understanding of the role of microcalcifications on the MPS in an atheroma plaque vessel.

Funding

This research was supported by the Spanish Ministry of Economy and Competitiveness through the research project DPI 2010-20746-C03-01, and the CIBER initiative. M.C. was supported by the Diputacion General de Aragon (DGA) through the grant B137/09.

References

1. Lloyd-Jones D, Adams R, Carnethon M, et al. Heart disease and stroke statistics—2009 update: a report from

the American Heart Association Statistics Committee and Stroke Statistics Subcommittee. *Circulation* 2009; 119: 21–181.
2. Hanke H, Lenz C and Finking G. The discovery of the pathophysiological aspects of atherosclerosis—a review. *Acta Chir Belg* 2001; 101: 162–169.
3. Ohayon J, Finet G, Treyve F, et al. A three dimensional finite element analysis of stress distribution in a coronary atherosclerotic plaque: in-vivo prediction of plaque rupture location. *Biomech Appl Comput Assist Surg* 2005; 17: 225–241.
4. Versluis A, Bank AJ and Douglas WH. Fatigue and plaque rupture in myocardial infarction. *J Biomech* 2006; 39: 339–347.
5. Virmani R, Kolodgie FD, Burke AP, et al. Lessons from sudden coronary death: a comprehensive morphological classification scheme for atherosclerotic lesions. *Arterioscler Thromb Vasc Biol* 2000; 20: 1262–1275.
6. Krishna Kumar R and Balakrishnan KR. Influence of lumen shape and vessel geometry on plaque stresses: possible role in the increased vulnerability of a remodelled vessel and the shoulder of a plaque. *Heart* 2005; 91: 1459–1465.
7. Cilla M, Peña E and Martinez MA. 3D computational parametric analysis of eccentric atheroma plaque: influence of axial residual stresses. *Biomech Model Mechanobiol* 2012; 11(7): 1001–1013.
8. Roijers RB, Dutta RK, Cleutjens JPM, et al. Early calcifications in human coronary arteries as determined with a proton microprobe. *Anal Chem* 2008; 80: 55–61.
9. Van der Giessen AG, Gijsen FJH, Wentzel JJ, et al. Small coronary calcifications are not detectable by 64-slice contrast enhanced computed tomography. *Int J Cardiovasc Imaging* 2011; 27(1): 143–152.
10. Friedrich GJ, Moes NY, Mühlberger VA, et al. Detection of intralesional calcium by intracoronary ultrasound depends on the histologic pattern. *Am Heart J* 1994; 128: 435–441.
11. Lee RT, Schoen FJ, Loree HM, et al. Circumferential stress and matrix metalloproteinase 1 in human coronary atherosclerosis. *Arterioscler Thromb Vasc Biol* 1996; 16(8): 1070–1073.
12. Kaazempur-Mofrad MR, Isasi AG, Younis HF, et al. Characterization of the atherosclerotic carotid bifurcation using MRI, finite element modeling, and histology. *Ann Biomed Eng* 2004; 32(7): 932–946.
13. Vengrenyuk Y, Carlier S, Xanthos S, et al. A hypothesis for vulnerable plaque rupture due to stress-induced debonding around cellular microcalcifications in thin fibrous caps. *Proc Natl Acad Sci USA* 2006; 103: 14678–14683.
14. Cheng G, Loree H, Kamm R, et al. Distribution of circumferential stress in ruptured and stable atherosclerotic lesions. A structural analysis with histopathological correlation. *Circulation* 1993; 87: 1179–1187.
15. Huang H, Virmani R, Younis H, et al. The impact of calcification on the biomechanical stability of atherosclerotic plaques. *Circulation* 2001; 103: 1051–1056.
16. Wong K, Thavornpattanapong P, Cheung S, et al. Effect of calcification on the mechanical stability of plaque based on a three-dimensional carotid bifurcation model. *BMC Cardiovasc Disord* 2012; 12(1): 7.
17. Bluestein D, Alemu Y, Avrahami I, et al. Influence of microcalcifications on vulnerable plaque mechanics using FSI modelling. *J Biomech* 2008; 41: 1111–1118.
18. Wenk JF, Papadopoulos P and Zohdi TI. Numerical modeling of stress in stenotic arteries with microcalcifications: a micromechanical approximation. *ASME J Biomech Eng* 2010; 132(9): 091011.
19. Wenk JF. Numerical modeling of stress in stenotic arteries with microcalcifications: a parameter sensitivity study. *ASME J Biomech Eng* 2011; 133: 014503.
20. Maldonado N, Kelly-Arnold A, Vengrenyuk Y, et al. A mechanistic analysis of the role of microcalcifications in atherosclerotic plaque stability: potential implications for plaque rupture. *Am J Physiol Heart Circ Physiol* 2012; 303(5): H619–H628.
21. Finet G, Ohayon J and Rioufol G. Biomechanical interaction between cap thickness, lipid core composition and blood pressure in vulnerable coronary plaque: impact on stability or instability. *Coron Artery Dis* 2004; 15: 13–20.
22. Lee R. Atherosclerotic lesion mechanics versus biology. *Zeitschrift fur Kardiologie* 2000; 89: 80–84.
23. Ohayon J, Finet G, Gharib AM, et al. Necrotic core thickness and positive arterial remodeling index: emergent biomechanical factors for evaluating the risk of plaque rupture. *Am J Physiol Heart Circ Physiol* 2008; 295: H717–H727.
24. Cilla M, Martinez J, Peña E, et al. Machine learning techniques as a helpful tool towards determination of plaque vulnerability. *IEEE Trans Biomed Eng* 2012; 9(4): 1155–1161.
25. Williamson SD, Lam Y, Younis HF, et al. On the sensitivity of wall stresses in diseased arteries to variable material properties. *ASME J Biomech Eng* 2003; 125: 147–155.
26. Li Z, Howarth S, Tang T, et al. Does calcium deposition play a role in the stability of atheroma? Location may be the key. *Cerebrovasc Dis* 2007; 24: 452–459.
27. Tang D, Yang C, Zheng J, et al. Quantifying effects of plaque structure and material properties on stress distributions in human atherosclerotic plaques using 3D FSI models. *ASME J Biomech Eng* 2005; 127: 1185–1194.
28. Sobol IM. Global sensitivity indices for nonlinear mathematical models and their Monte Carlo estimates. *Math Comput Simulat* 2001; 55: 271–280.
29. Davies MJ. Stability and instability: two faces of coronary atherosclerosis: the Paul Dudley White lecture 1995. *Circulation* 1996; 94: 2013–2020.
30. Ohayon J, Teppaz P, Finet G, et al. In-vivo prediction of human coronary plaque rupture location using intravascular and finite element method. *Coron Artery Dis* 2001; 12: 655–663.
31. Fujii K, Carlier SG, Mintz GS, et al. Association of plaque characterization by intravascular ultrasound virtual histology and arterial remodeling. *Am J Cardiol* 2005; 96: 1476–1483.
32. Roy CS. The elastic properties of the arterial wall. *J Physiol* 1881; 3(2): 125–159.
33. Patel DJ and Fry DL. The elastic symmetry of arterial segments in dogs. *Circ Res* 1969; 24(1): 1–8.
34. Cox RH. Passive mechanics and connective tissue composition of canine arteries. *Am J Physiol* 1978; 234(5): 533–541.
35. Holzapfel GA, Gasser CT, Sommer G, et al. Determination of the layer-specific mechanical properties of human coronary arteries with non-atherosclerotic intimal thickening, and related constitutive modelling. *Am J Physiol Heart Circ Physiol* 2005; 289: H2048–H2058.
36. Carew TE, Vaishnav RN and Patel DJ. Compressibility of the arterial wall. *Circ Res* 1968; 23: 61–86.

37. Chuong CJ and Fung YC. Compressibility and constitutive equation of arterial wall in radial compression experiments. *J Biomech* 1984; 17(1): 35–40.
38. Gasser TC, Ogden RW and Holzapfel GA. Hyperelastic modelling of arterial layers with distributed collagen fibre orientations. *J R Soc Interface* 2006; 3: 15–35.
39. Spencer AJM. Theory of invariants. In: *Continuum physics*. AC Eringen (Ed) New York: Academic Press, 1971, pp.239–253.
40. Marquardt DW. An algorithm for least-squares estimation of nonlinear parameters. *SIAM J Appl Math* 1963; 11: 431–441.
41. Loree HM, Grodzinsky AJ, Park SY, et al. Static circumferential tangential modulus of human atherosclerotic tissue. *J Biomech* 1994; 27: 195–204.
42. Lendon CL, Davies MJ, Born GVR, et al. Atherosclerotic plaque caps are locally weakened when macrophages density is increased. *Atherosclerosis* 1991; 87: 87–90.
43. Lee RT, Loree HM and Fishbein MC. High stress regions in saphenous vein bypass graft atherosclerotic lesions. *J Am Coll Cardiol* 1994; 24(7): 1639–1644.
44. Beattie D, Xu C, Vito R, et al. Mechanical analysis of heterogeneous, atherosclerotic human aorta. *ASME J Biomech Eng* 1998; 120: 602–607.
45. Holzapfel GA, Stadler M and Schulze-Bauer CAJ. A layer specific three-dimensional model for the simulation of balloon angioplasty using magnetic resonance imaging and mechanical testing. *Ann Biomed Eng* 2002; 30: 753–767.
46. Holzapfel GA, Sommer G and Regitnig P. Anisotropic mechanical properties of tissue components in human atherosclerotic plaques. *ASME J Biomech Eng* 2004; 126: 657–665.
47. Kiousis DE, Rubinigg SF, Auer M, et al. A methodology to analyze changes in lipid core and calcification onto fibrous cap vulnerability: the human atherosclerotic carotid bifurcation as an illustratory example. *ASME J Biomech Eng* 2009; 131(12): 121002.
48. Arroyo LH and Lee RT. Mechanisms of plaque rupture: mechanical and biologic interactions. *Cardiovasc Res* 1999; 41: 369–375.
49. Briley-Saebo KC, Mulder WJM, Mani V, et al. Magnetic resonance imaging of vulnerable atherosclerotic plaques: current imaging strategies and molecular imaging probes. *J Magn Reson Imaging* 2007; 26: 460–479.
50. Armentano R, Megnien JL, Simon A, et al. Effects of hypertension on viscoelasticity of carotid and femoral arteries in humans. *Hypertension* 1995; 26: 48–54.
51. Peña E, Alastrue V, Laborda A, et al. A constitutive formulation of vascular tissue mechanics including viscoelasticity and softening behaviour. *J Biomech* 2010; 43: 984–989.
52. Saito GE and Werff TJ. The importance of viscoelasticity in arterial blood flow models. *J Biomech* 1975; 8(3–4): 237–245.
53. Alastrue V, Peña E, Martinez MA, et al. Assessing the use of the "opening angle method" to enforce residual stresses in patient-specific arteries. *Ann Biomed Eng* 2007; 35: 1821–1837.
54. Ohayon J, Dubreuil O, Tracqui P, et al. Influence of residual stress/strain on the biomechanical stability of vulnerable coronary plaques: potential impact for evaluating the risk of plaque rupture. *Am J Physiol Heart Circ Physiol* 2007; 293: H1987–H1996.
55. Kock SA, Nygaard JV, Eldrup N, et al. Mechanical stresses in carotid plaques using MRI-based fluid-structure interaction models. *J Biomech* 2008; 41: 1651–1658.
56. Himburg HA, Grzybowski DM, Hazel AL, et al. Spatial comparison between wall shear stress measures and porcine arterial endothelial permeability. *Am J Physiol Heart Circ Physiol* 2004; 286: H1916–H1922.
57. Raggi P, Callister TQ, Cooil B, et al. Identification of patients at increased risk of first unheralded acute myocardial infarction by electron-beam computed tomography. *Circulation* 2000; 101: 850–855.